The 14th World Conference on Earthquake Engineering
October 12-17, 2008, Beijing, China

SOFTENING BEHAVIOR OF RC COLUMNS UNDER CYCLIC LOADING

Jung-Yoon Lee[1], Susumu Kono[2], Fumio Watanabe[3], and Yeon-Geol Cheong[4]

[1] *Associate Professor, Department of Architectural Engineering, Sungkyunkwan University, South-Korea, jylee@skku.ac.kr*
[2] *Associate Professor, Dept. of Architecture and Architectural Engineering, Kyoto University, Japan, (Katsura, Nishikyo-ku, Kyoto, 615-8540, Japan, E-mail : kono@archi.kyoto-u.ac.jp)*
[3] *Professor, Dept. of Architecture and Architectural Engineering, Kyoto University, Japan, (Katsura, Nishikyo-ku, Kyoto, 615-8540, Japan, E-mail : nabe@archi.kyoto-u.ac.jp)*
[4] *Graduate student, Department of Architectural Engineering, Sungkyunkwan University, South-Korea*

ABSTRACT :

The load carrying capacity and energy dissipation behavior of columns in post yield range of deformation has a significant role to prevent a total collapse of reinforced concrete buildings. Reinforced concrete short (small height to depth ratio) column dominated by shear generally indicates the reduction of lateral load capacity and less energy dissipation due to pinching effect after peak load. Therefore the seismic design of RC short columns needs to consider not only the shear strength but also the post peak behavior in view of capacity reduction and energy dissipation during load cycling. However there are few researches on the post peak behavior of shear dominated short column.
Ten RC columns with varying shear reinforcement ratios and axial force ratios were tested under reversed cyclic loading. Test results indicated that the nominal concrete contribution to shear resistance in the plastic hinge region decreased after flexural yielding of the column. In addition, the axial force decreased the deformability of RC members, but eliminated the pinching effect in the post-yield load hysteretic response.

KEYWORDS: RC columns, axial strain, deformability, load patterns, axial load, pinching effect

1. INTRODUCTION

The usual earthquake resistant design philosophy of ductile frame buildings allows the beams to form plastic hinges adjacent to beam-column connections. To complete the plastic deformation mechanism, however, column plastic hinges at the base of the structure are also required. With bridges it is neither feasible nor desirable to locate the plastic hinges in the superstructure, and thus, the columns tend to be the prime source of energy dissipation. In order to carry out this design philosophy, the ultimate shear strength of the column should be greater than the flexural yielding force and should not degrade before reaching its required ductility.
Special care is needed when a plastic hinge forms in column at the base of the structure because of its relatively short-span-to-depth ratio. After flexural yielding, a plastic hinge develops at the bottom of the column, followed by yielding of the shear reinforcement and crushing of the diagonal compressive concrete struts in the plastic hinge regions, which led to a sudden failure of the column. The deformability of this column is relatively small when compared to the deformability of column with a larger span-to-depth-ratio. Thus the design of RC columns with short-span-to-depth ratios under reversed cyclic loadings necessitates the prediction of both the shear strength after flexural yielding and the corresponding ductility of such structural members.
Nevertheless, most of the research done on the shear behavior of RC columns has been previously carried out with the purpose of predicting the shear strength of the column and no emphasis has been placed on the column's ductility or shear failure modes. Accordingly, the objective of this paper is to predict the deformability of shear dominated RC columns after yielding of the main flexural steel.
ACI (2005) and AIJ (1999) codes place a priority in the prediction of the shear strengths of RC members and indirectly allows for the ductile capacity by providing some conservatism in the calculation of the shear strength of the concrete. A design guideline proposed by AIJ (1990) evaluates the shear strengths of RC members by combining the shear contribution of the steel reinforcement by considering a truss mechanism to the concrete

contribution considering an arch mechanism based on the lower bound plastic theory. Furthermore, the ductile capacity is accounted for by limiting the inclination of the concrete strut in the truss model and imposing deterioration in the effective compressive strength of the cracked concrete. Unfortunately, this current guideline is not successful in predicting the observed ductile capacities of RC columns with reasonable accuracy (Lee and Watanabe, 2003a) because the assumed limitations overestimate the shear strength deterioration of concrete in the plastic hinge regions. Priestley et al. (1996) proposed a shear strength design approach for RC columns under cyclic load. In this approach, the shear strength of concrete reduced with increasing of the deformability of columns.
To design earthquake-resistant shear-dominated RC columns, it is necessary to know not only the shear strength but also the ductility of these members. The research reported in this paper provides the test results of RC columns with short-span-to-depth-ratios failing in shear after flexural yielding.

2. TEST PROGRAM

2.1 Test Specimens

The experimental program consisted of ten RC columns having different shear reinforcement ratios. The ten columns were divided into four groups depending on the loading patterns and shear reinforcement ratios. As listed in Table 1, a monotonic loading was applied to the specimen in Group-1(M-00, -15, and -30), half-reversed cyclic loading to the specimens in Group-2 (C1-15 and -30), and full-reversed cyclic loading to the specimens in Group-3 and -4. Each group consisted of two or three specimens having different axial load ratios of the columns (n): 0%, 15.0%, and 30.0%. The specimens in Group-3 and Group-4 were designed to be applied to the same axial load but have different shear reinforcement ratios (ρ_w) . The ρ_w for the specimens in Group-3 was 0.42%, while that for the specimens in Group-4 was 0.63%.
All of the test columns were designed to fail due to concrete crushing in the plastic hinges after flexural yielding. The potential shear strength ratio ($V_{n\text{-}aci}$ / $V_{,f}$, in which $V_{n\text{-}aci}$: shear strength calculated by ACI 318-05 code, $V_{,f}$: shear strength at flexural yielding) varied from 1.23 to 2.46. The average concrete cylinder strength of each specimen at the time of test was 27.62 MPa (4,004 psi). Other material properties of test specimens are listed in Table 1.

2.2 Testing Method and Measurements

The cross section of the beams was 250 mm square as shown in Fig. 1. The core size, measured from center-to-center of the perimeter hoops, was 170 x 170mm (6.69 x 6.69 in.) for all specimens. The overall length of the beams was 1,450 mm (57.09 in.), and the 430 mm (16.93 in.) long of the columns was designed as the test region.

Table 1 Material properties of RC columns

Columns		f_c ' (MPa)	Shear reinforcement				Longitudinal tensile reinforcement				n (%)	Loading Patterns	V_{n-aci} (kN)	V_f (kN)	V_{n-aci} / V_f
			s (mm)	ρ_t (%)	A_t (mm^2)	f_{ty} (MPa)	n (ea.)	A_w (mm^2)	ρ_w (%)	f_{ly} (MPa)					
G-1	M-00	27.37	60	0.42	31.6	330.0	3	198.6	1.13	322.4	0	M	117.6	62.7	1.88
	M-15	27.47	60	0.42	31.6	330.0	3	198.6	1.13	322.4	15	M	129.1	92.0	1.40
	M-30	28.02	40	0.42	31.6	330.0	3	198.6	1.13	322.4	30	M	140.6	114.0	1.23
G-2	C1-15	27.47	60	0.42	31.6	330.0	3	198.6	1.13	322.4	15	C1	129.1	92.0	1.40
	C1-30	28.02	60	0.42	31.6	330.0	3	198.6	1.13	322.4	30	C1	140.6	114.0	1.23
G-3	C2-00S	27.37	60	0.42	31.6	330.0	3	198.6	1.13	322.4	0	C2	117.6	62.7	1.88
	C2-15S	27.47	60	0.42	31.6	330.0	3	198.6	1.13	322.4	15	C2	129.1	92.0	1.40
G-4	C2-00L	27.37	40	0.63	31.6	330.0	3	198.6	1.13	322.4	0	C2	154.1	62.7	2.46
	C2-15L	27.47	40	0.63	31.6	330.0	3	198.6	1.13	322.4	15	C2	165.6	92.0	1.80
	C2-30L	28.02	40	0.63	31.6	330.0	3	198.6	1.13	322.4	30	C2	177.1	114.0	1.55

G-group, M: monotonic loading, C1: two half-reversed cyclic loading, C2: two full-reversed cyclic loading

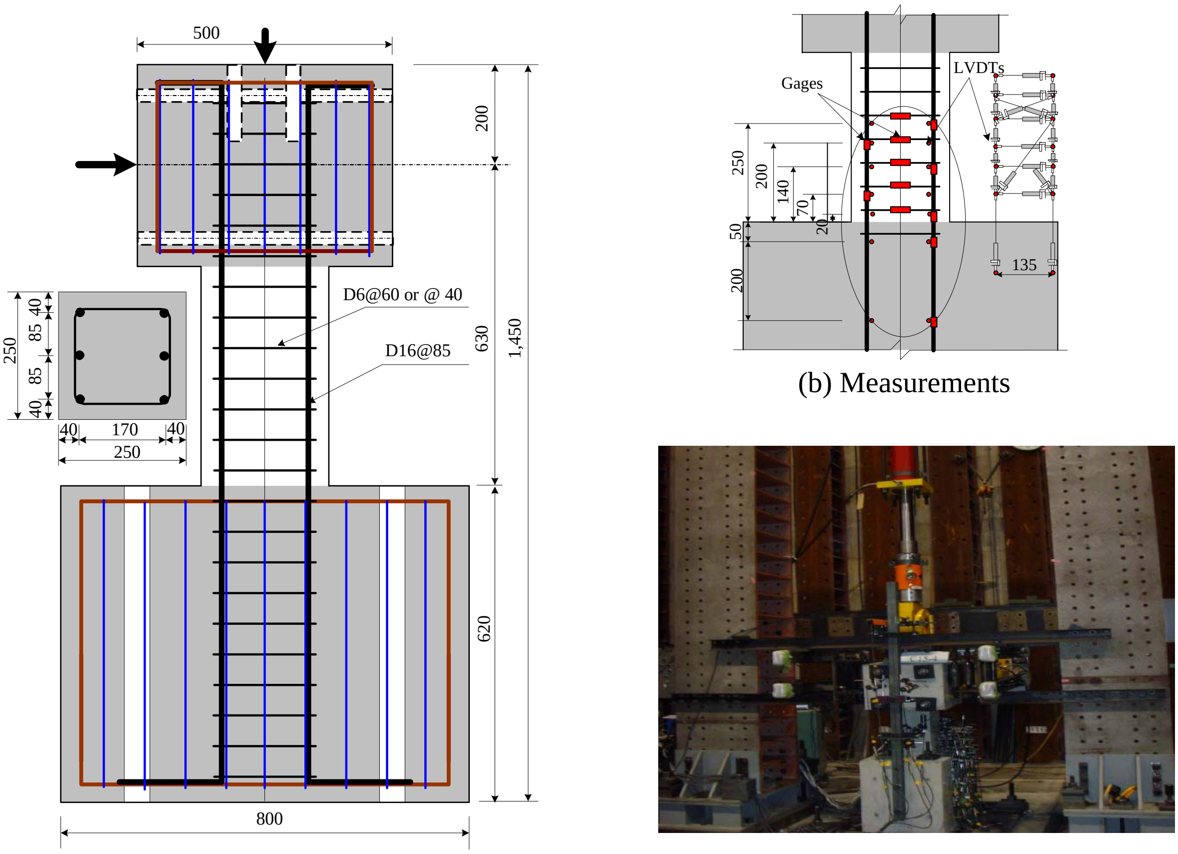

(a) Overall dimensions of specimens (unit : mm)

(b) Measurements

(c) Loading system

Figure 1 Overall dimensions of specimen and loading system

Heavier reinforcement was placed outside the test region to prevent premature failure in the stub zones. The 192 x192 mm (7.56 x 7.56 in.) closed stirrup was fabricated for use as the shear reinforcement in the transverse direction. Accounting for relatively short shear span-to-depth ratio of the columns at the base of the RC structures, the shear-span-to-depth ratio of all specimens was designed to be 3. The specimens were supported in vertical position, and quasi-static cyclic lateral load was applied at the top of the column using a servo-controlled hydraulic actuator. Lateral cyclic load was applied under displacement control by a horizontal actuator with the displacement capacity of ± 400 mm. To prevent the displacement in out-of-plane direction, four rollers were placed as shown in Fig. 1(c). The test was terminated when the resisting force in the post-peak load-deformation curve dropped to about 80% of the peak-recorded strength.

Twenty linear displacement transducers (LVDTs) were attached to the face of the plastic hinge region of the test column to measure curvature, longitudinal and transverse axial deformation as well as shear deformation as shown in Fig. 1(b). Two LVDTs were attached to the face of the base stub to measure the axial elongation in the stub. Nine LVDTs were attached to both sides of the columns to measure the angle of rotation, the deflection, and P-delta effect. In addition, the strains of the transverse and longitudinal steel bars in the test region were measured by strain gauges attached on the surface of the steel bars. The placements of strain gauges and LVDTs installed for the measurements are shown in Fig. 1(b).

3. TEST RESULTS

3.1 Overall behavior

All of the columns failed after flexural yielding occurred. Cracks and concrete spalling were mostly observed at the plastic hinge region. For all specimens, the failure was caused by concrete crushing in the plastic hinge regions. In case of the specimens without axial load, M-00, C2-00S, and C2-00L, a plastic hinge developed near

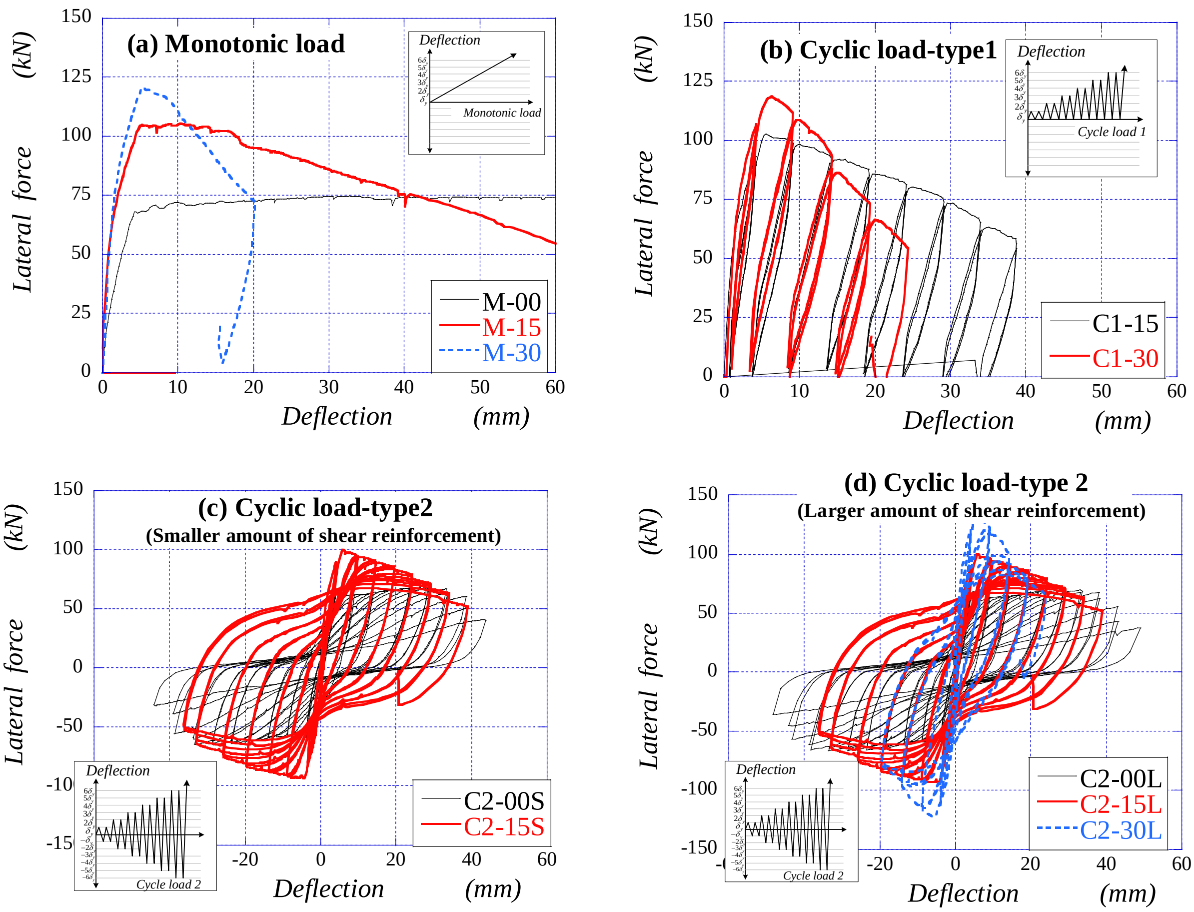

Figure 2 Lateral force vs. deflection curves of test specimens

the base of the specimen; then, the shear reinforcement yielded and the diagonal compressive concrete struts crushed in the plastic hinge regions, which led to a sudden failure of the beam. The energy dissipation of these specimens was relatively small due to the pinching effects when compared to the energy dissipation of a similar column. For the column specimens, tested under the axial ratio of 15% or 30%, the cover concrete spalled off in the plastic hinge region after the flexural tensile steel bars reached their yield strains. The longitudinal bar buckling was not observed in all specimens. Specimen M-00 was terminated when the deflection reached 82mm due to the limitation of the displacement capacity of test facility.

3.2 Discussion of test results

Figure 2 shows the experimental observation of the lateral force versus deflection curves for the test specimens. The deformability of specimens decreased with increasing of the axial load, while the flexural yield strength of specimens increased with increasing of the axial load. For example, the flexural yielding capacity of Specimen M-30 was 120.8 kN, while that of Specimen M-00 was 74.6 kN. The deflection corresponding to $0.8V_{max}$ (V_{max} is the maximum-recorded load) of Specimen C2-30L, tested under high axial load (n=30%), was 13.33mm, while that of Specimen C2-15L, tested under low axial load (n=15%), was 23.67mm.

[Effect of loading patterns]

To study the effect of loading history on the behavior of RC members, Group-1, -2, and -3 were tested under three different types of loading patterns, respectively. For the specimens under no axial load, the observed deformability (deflection) of specimen M-00, tested under monotonic load, was much greater than that of Specimen C2-00S, tested under full-reversed cyclic loading. However, the loading patterns did not influence on the deformability of

Specimens tested under high axial load so much as that of Specimens tested low axial load. The deformability of Specimen C, tested under monotonic lateral load and high axial load, was little greater than that of C2-30L, tested under full-reversed lateral cyclic loading and high axial load. This issue is discussed in details in a subsequent section.

[Longitudinal axial strain]

Lee and Watanabe (2003b) indicated that the longitudinal axial strain in the plastic hinge regions of RC structures had a significant influence on the behavior of RC structures subjected to reversed cyclic loading. The elongation in the plastic hinge affected the deformability and energy dissipation in the hysteretic response by decreasing the effective compressive strength of cracked concrete of the RC members dominated by shear action. To study the relationship between longitudinal axial strain and deformability, the experimental observations of the longitudinal axial strain versus deflection curves for the test specimens were compared in Fig. 3. The longitudinal axial strain is the average value of the strains in the compressive and tensile steel bars which were measured by LVDTs attached to the face of the plastic hinge region of the test specimens. The axial strain versus deflection curve of beam specimens (M-00, C2-00S, and C2-00L) consists of four strain paths as shown in Fig. 3. A similar observation was reported by Lee and Watanabe (2003b) from the test results of twelve RC beams. Four strain paths are summarized below:

Path 1: Pre-flexural yielding or unloading region; the rate of decrease of the longitudinal axial strain in the unloading region is the same as the increasing rate of the axial strain in the elastic region.

Path 2: Post-flexural yielding region; the longitudinal axial strain, ε_x, in the plastic hinge region increases rapidly as the rotation increases beyond flexural yielding.

Path 3: Slip region; the change in ε_x is negligible.

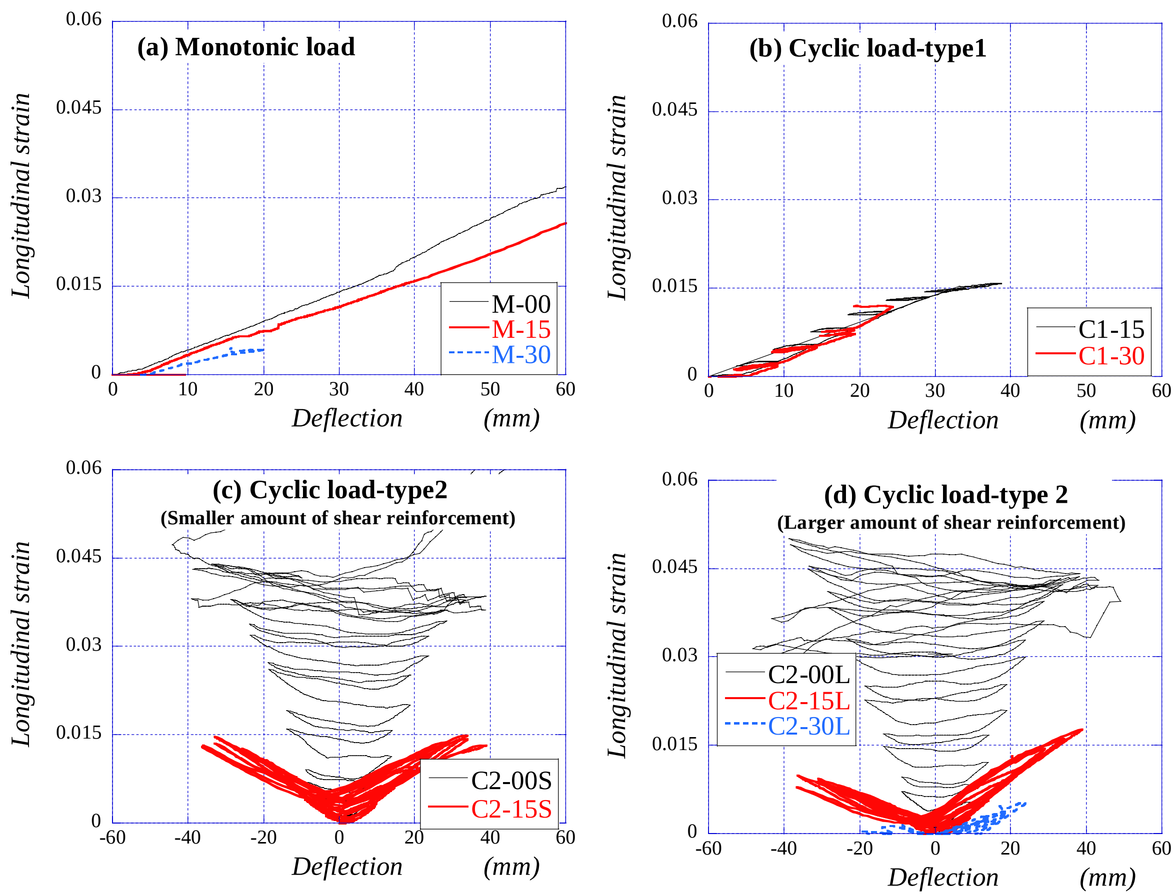

Figure 3 Longitudinal axial strain vs. deflection curves of test specimens

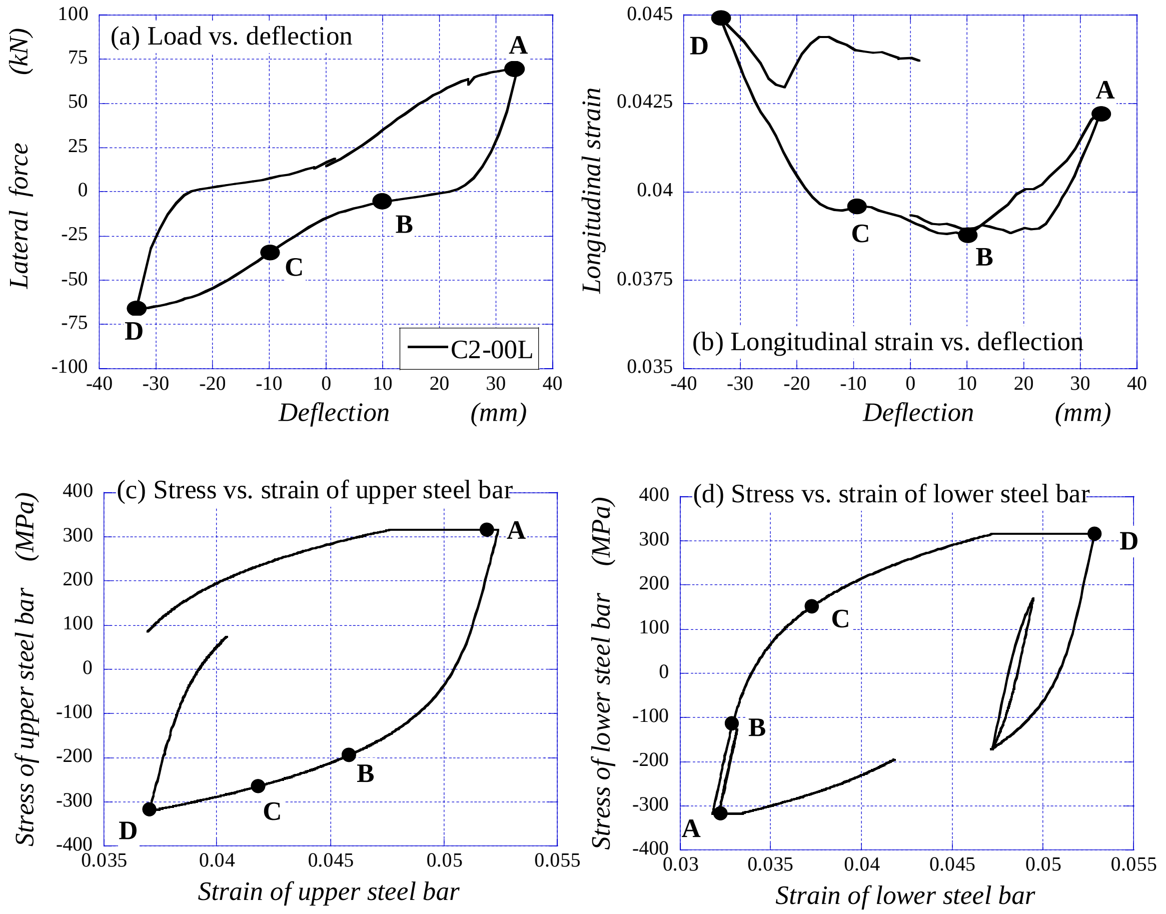

Figure 4 One cycle of hysteresis for C2-00L

Path 4: Repeated loading region; the increase in the magnitude of axial strain, ε_x, is inversely proportional to the number of reloading cycles.

However, the axial strain versus deflection curve of column specimens consists of two strain paths as shown in Fig. 3. The longitudinal axial strain in post-flexural yielding region of column specimens was almost the same to the strain in pre-flexural yielding region. In addition, the slip region in which the axial strain remains constant as the deflection direction of the member changes is barely observed in the strain-deflection relationship of column specimens. Figure 3 shows that the longitudinal axial strain decreases as the axial load increases. For example, the axial strains at the deflection of 20mm of M-00(no axial load), M-15(n= 15%), and M-30(n=30%) were 0.009, 0.0074, and 0.0043, respectively.

[Slip region and pinching mechanism]

The main difference of longitudinal axial strains between beam and column specimens was the slip region. The longitudinal axial strain vs. deflection curves of beam specimens, C2-00S and C2-00L, have the slip region, while those of column specimens have not as shown in Fig. 3. The slip of longitudinal axial strain has a significant influence on the behavior of RC structures subjected to reversed cyclic loading. The slip in the plastic hinge region reduces energy dissipation in the post-yield load hysteretic response due to pinching effect.

The test results of C2-00L (no axial load) are considered to study the presence of the slip region and pinching effect. Fig. 4(a) shows the first cycle of the hysteretic loop at the deflection of $\pm 33mm$ in terms of the lateral force vs. deflection. Fig. 4 (b) shows the corresponding longitudinal axial strain-deflection curves of the specimen, while Fig. 4 (c) and (d) show the corresponding stress-strain curves of the upper and lower steel bars, respectively. To correlate the lateral forces and deflections to the stresses and strains in the steel bars, four points A, B, C, and D are chosen in Fig. 4(a) and the corresponding points are designated in Fig. 4(b), (c) and (d). Point A is at the maximum positive deflection of the hysteretic loop. Point B is at the stage where the lateral force is almost zero after unloading. Point C is taken in the negative strain region at the end of the low-stress pinching zone just before the sudden increase in stiffness. Point D is at the maximum negative deflection of the hysteretic loop.

As the specimen C2-00L is unloaded from point A to point B in Fig. 4(a), the stress of the upper steel bar also is reduced from the maximum tensile stress to compressive stress, Fig. 4(c). Correspondingly, the stress of the lower steel bar is unloaded from a maximum negative(compressive) value of -322.4MPa to a smaller negative value of -113.0MPa, Fig. 4(d). In this unloading stage, the cracks are closing from a very large width to a much smaller width under a negligible concrete stress. During this unloading stage, all the equilibrium as well as compatibility equations are satisfied. As the load-deflection curve proceeds from point B to point C, Fig 4(a), the strain of upper steel bar decreases from 0.0458 to 0.0418, Fig. 4(c), representing the closing of the upper cracks due to a reducing upper strain. At the same time, the strain of lower steel bar increases from 0.0328 to 0.0373, Fig. 4(d), representing an opening of the lower cracks. From compatibility, these two strains (upper and lower) produce a large change in the strains from 0.0045 to -0.004. From equilibrium, the small stresses in the steel bars produce a small lateral load. In other words, the beam is offering very small lateral load resistance to a very large deflection. This phenomenon characterizes the pinching effect.

The test results of C2-15L are analyzed to illustrate the absence of a pinching mechanism when high axial load is applied. Fig. 5 (a) shows the first cycle of the hysteretic loop at the deflection of $\pm 33mm$ in terms of the lateral force vs. deflection. Fig. 5 (b) shows the corresponding longitudinal axial strain-deflection curves of the specimen, while Fig. 5 (c) and (d) show the corresponding stress-strain curves of the upper and lower steel bars, respectively. As the element is unloaded from point A to point B in Fig. 5(a), the lateral load is reduced from 67.6 kN to -26.0

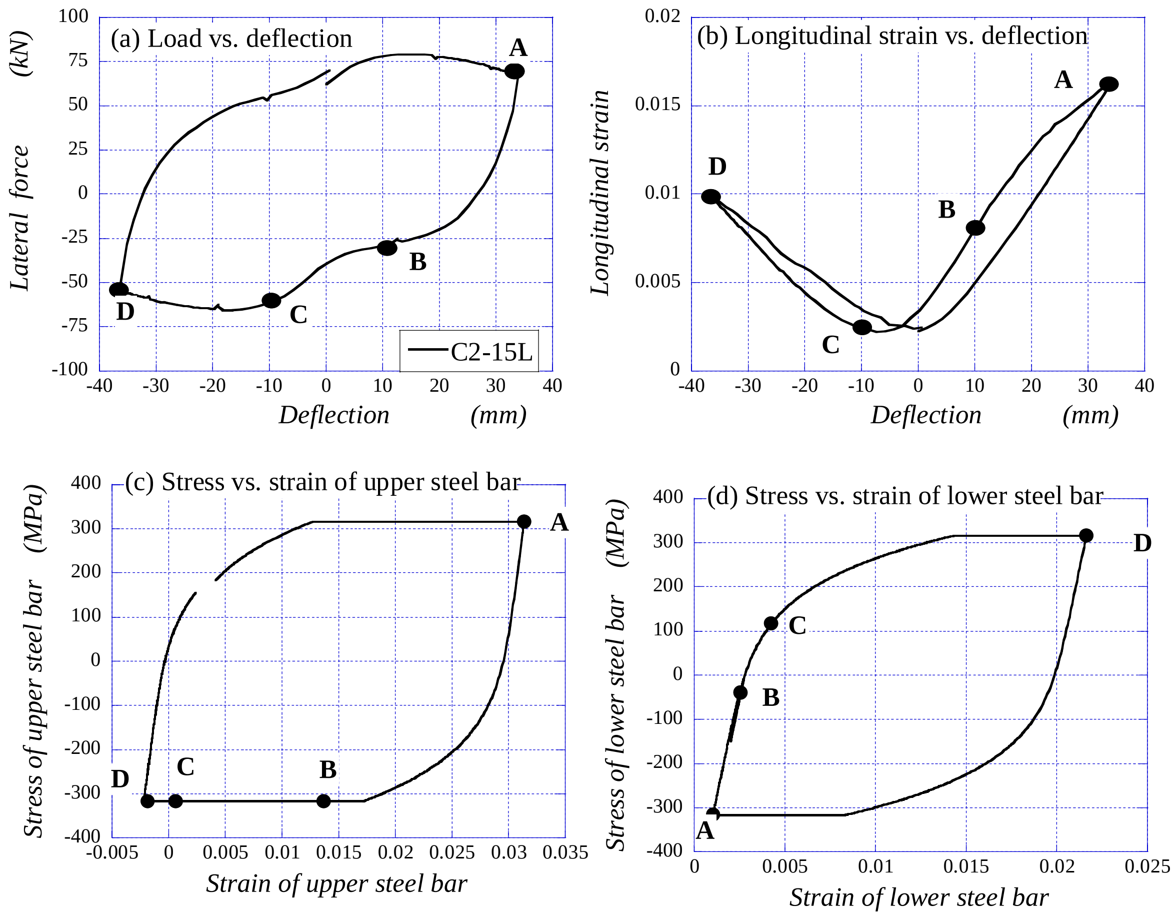

Figure 5 One cycle of hysteresis for C2-15L

kN. The stress of upper steel bar also is reduced from the maximum tensile stress (322.4 MPa) to maximum compressive stress (-322.4 MPa) as shown in Fig. 5(c), while the stress of lower steel bar is increased from the maximum compressive stress (-322.4 MPa) to -39.3 MPa as shown in Fig. 5(d).

As the load of C2-15L, tested under high axial load, proceeds from point B to point C, the axial strain decreases toward the compressive strain as shown in Fig. 5(b). This is because the strain of upper steel bar from point B to point C produces a large change in the strains from 0.0136 to 0.00062, while that of lower steel bar from 0.0136 to 0.00062 as shown in Fig. 5(d). Therefore, the longitudinal axial strain versus deflection curve does not show the slip region, Fig. 5(b.

Because of high axial load, the stress at point B of C2-15L is much greater than that of C2-00L. From equilibrium, the large steel stresses produce a large jump in the lateral load from -29.0 MPa at point B to –61.4 MPa at point C (Fig. 5(a)). In other words, the column is offering a high load stiffness from point B to point C (Fig. 5(a)). This phenomenon characterizes the absence of the pinching mechanism.

4. CONCLUSIONS

In this paper, ten RC columns with varying shear reinforcement ratios and axial force ratios were tested under reversed cyclic loading to assess the effect of the axial load on the deformability and "pinching effect" for the hystertic loops of the lateral force and deflection curves. Test results showed that the axial force decreased the deformability of RC members, but eliminated the pinching effect in the post-yield load hysteretic response. In addition, the longitudinal axial strain in the plastic hinge region decreased as the axial load increased. The axial strain versus deflection curve of beam specimens consisted of four strain paths, while that of column specimens consisted of only two paths. The slip region was barely observed in the strain-deflection relationship of column specimens.

REFERENCES

ACI Committee 318-05 (2005). Building Code and Commentary. American Concrete Institute, USA.

Architectural Institute of Japan (1990). Design Guidelines for Earthquake Resistant Reinforced Concrete Buildings Based on Ultimate Strength Concept. Architectural Institute of Japan, Japan.

Architectural Institute of Japan (1999). Standard for Structural Calculation of Reinforced Concrete Structures. Architectural Institute of Japan, Japan.

Lee, J.-Y. and Watanabe F. (2003a). Shear Deterioration of Reinforced Concrete Beams Subjected to Reversed Cyclic Loading. *ACI Structural Journal* **100: 4**, 480-489.

Lee, J.-Y. and Watanabe F. (2003b). Predicting the Longitudinal Axial Strain in the Plastic Hinge Regions of Reinforced Concrete Beams Subjected to Reversed Cyclic Loading. *Engineering Structures* **25: 7**, 927-939.

Priestley, M.J.N., Seible, F. and Calvi, G. M. (1996). Seismic Design and Retrofit of Bridges. A Wiley-Interscience Publication.